Journal of Photochemistry and Photobiology A: Chemistry 222 (2011) 366–369

Contents lists available at ScienceDirect

Journal of Photochemistry and Photobiology A: Chemistry

journal homepage: www.elsevier.com/locate/jphotochem

Short Note

# Indoline-dye immobilized ZnO nanoparticles for whopping 5.44% light conversion efficiency

Swapnil B. Ambade[a], Rajaram S. Mane[b,d], Sung-Hwan Han[b], Soo-Hyoung Lee[a,*], Myung-Mo Sung[b], Oh-Shim Joo[c,**]

[a] Organic Optoelectronic Materials Laboratory, Division of Semiconductor and Chemical Engineering, Chonbuk National University, Jeonju, Republic of Korea
[b] Inorganic Nanomaterials Laboratory, Department of Chemistry, Hanyang University, Seoul, Republic of Korea
[c] Clean Energy Research Center, Korea Institute of Science and Technology, Seoul 130-650, Republic of Korea
[d] School of Physical Sciences, Swami Ramanand Teerth Marathwada University, Nanded, India

ARTICLE INFO

*Article history:*
Received 23 November 2010
Received in revised form 26 April 2011
Accepted 23 May 2011
Available online 14 June 2011

*Keywords:*
ZnO NPs
Indoline dye
*J–V*
Impedance
IPCE

ABSTRACT

Using indoline D102-dye, a whopping 5.44% light-to-electrical conversion efficiency owing to higher current density and open circuit voltage is explored for the ZnO nanoparticles (NPs)-based photoelectrode. The ZnO NPs/D102 dye structure has been designed onto indium-tin-oxide, electrons extractor, conducting and transparent substrate. The ZnO NPs of minimum [0 0 2] direction orientation compared to that of [1 0 0] and [1 0 1] directions, an indication of good charge transporting ability, with agglomerated grains of about 5–10 nm in diameters were immobilized in D102 dye for 1 h for dye loading. Low charge transport resistance and nearly 60% incident photon-to-current conversion efficiency were obtained. The results suggest that D102 dye can be potentially used for obtaining high performance ZnO-based dye-sensitized nanostructured solar cells.

© 2011 Elsevier B.V. All rights reserved.

## 1. Introduction

As the incessant quest for clean, sustainable, alternative renewable energy gathers enormous euphoria within the scientific community, interest of researchers and industrialists in solar photovoltaic cells is increasing progressively. In the search of a promising photoelectrode, dye-sensitized nanostructured solar cells (DNSCs)-based on nanostructured metal oxides including $TiO_2$, ZnO, $SnO_2$, etc., with a prospect of low-cost photovoltaic energy conversion, have attracted much attention in recent years [1–4] wherein, photo-excitation takes place in the dye molecules, and the photo-generated charges are then separated at the dye/oxide interface, and therefore, electrons are injected into the conduction band of semiconductor oxide, then diffuse through the semiconductor oxide to the collecting electrode. Surface area and the nanostructure of preferred wide band gap metal oxides and extinction coefficients of sensitizing dyes are essentially and critically important to get higher light-harvesting efficiency for higher solar-to-electrical conversion efficiency. The electron transport in the semiconductor oxide is dominated by diffusion; therefore, it is necessary to reduce the charge traps in the semiconductor oxides for enhancing electron transport kinetics to obtain higher current density and minimum recombination centers. Different proposed alternatives include the use of wider band gap energy metal oxides as capping layers or blocking layers for stopping reverse electrons, hopping-free one dimensional nanostructures and cocktail dyes [5,6], etc. In spite of novelty in nanostructure on account of its ease of crystallization and anisotropic growth, high direct band gap energy, high exciton energy, ZnO is one of the mostly suffered metal oxides. Very few groups have succeeded so far in achieving more than 5% light conversion efficiency based on ZnO nanostructures [7–9]. The factors that determine the efficiency of DNSCs are the photocurrent density ($J_{sc}$), the open circuit potential ($V_{oc}$), fill factor (*ff*), and the intensity of the incident light ($J_{sc}$) [10]. In general, the $J_{sc}$ and $V_{oc}$ are related to the rate of electron injection to the photoelectrode and the energy difference between the Fermi level of the photoelectrode and the Nernest potential of the redox couple in the electrolyte, respectively. Recent studies conclude that the $J_{sc}$ and $V_{oc}$ are greatly influenced by the number of carboxylic groups (protons) existing in the dye to anchor the photoelectrode and therefore, so far such investigations dealing with the relationship between the molecular structures of the dyes and the $J_{sc}$ and $V_{oc}$ were subjected to the ruthenium-based N3 dye and its derivatives, such as N749 and N719, which are characterized by as high as four protons per molecule [11,12]. Using a dye of relatively high

* Corresponding author.
** Corresponding author. Tel.: +82 29585215; fax: +82 29585219.
*E-mail addresses:* shlee66@jbnu.ac.kr (S.-H. Lee), joocat@kist.ac.kr (O.-S. Joo).

1010-6030/$ – see front matter © 2011 Elsevier B.V. All rights reserved.
doi:10.1016/j.jphotochem.2011.05.021

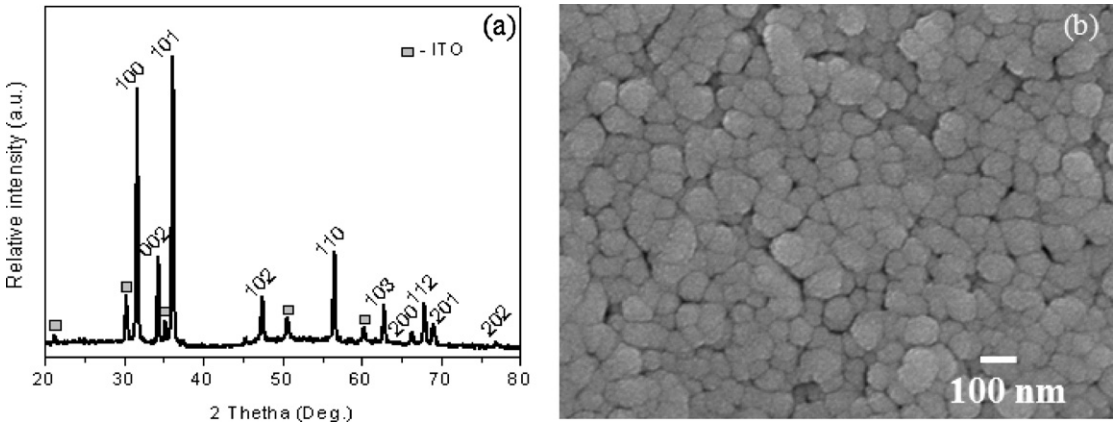


**Fig. 1.** (a) X-ray diffraction pattern confirming the formation of ZnO and (b) the SEM image revealing the nanometer sized angular grains.

extinction coefficient of minimum surface aggregation impact and CdS NPs immobilization for dual photosensitization, DNSCs performance of ZnO NPs-based electrodes can be improved immensely [13–15]. However, the variations observed in the $V_{oc}$ and $J_{sc}$, and therefore, efficiency of DNSCs constituted with metal-free organic dyes having a single carboxylic group [16–21], have not been explored to a larger extent. In this communication, ZnO NPs-based DNSCs using an indoline D102 dye is explored. In brief, structural and morphological aspects of ZnO NPs are presented in the preceding part and in the later; Nyquist plot obtained from impedance spectroscopy measurement, incident photon-to-current collection efficiency (IPCE), and the $J_{sc}$ and $V_{oc}$ characteristics are investigated. The D102 dye structure (inexpensive on account of its ruthenium free structure), commercially available, was used for immobilizing ZnO NPs electrodes of different thicknesses for optimal performance.

## 2. Experimental details

Nanostructured ZnO NPs electrodes of various thicknesses were prepared by application of NPs dispersion, obtained from Alfa Aesar, Germany, onto indium-tin-oxide (ITO) conducting and transparent substrate by spin method. The ZnO-solvent solution was filtered to remove dust, typically with a 0.45 μm filter before spinning. The plate is spun in at least two stages by simple spin-coating apparatus. During the first stage, the plate is spun at a low to moderate speed of 500–1000 rpm for 5–10 s to evenly spread the solution. In brief, ZnO electrodes deposited onto ITO were prepared from commercial ZnO paste composed of nanoparticles with approximate nanoparticle size of 20 nm and wurtzite structure (discussed later). The paste was mixed with 30% water and stirred overnight to obtain a colloidal suspension of ZnO. The thickness of the coating is then determined and controlled during the second stage by spinning the coating at a higher speed, between 1500 and 3000 rpm for anywhere between a few seconds and a minute. The ZnO NPs films of 2, 4, 6, 8, 10 (±0.2) μm were prepared. A Sloan Dectak profilometer was used to measure the thicknesses of all films. These were further annealed at 573 K for 60 min to remove organic contents, if any, and to improve the crystallinity, respectively. The X-ray diffractometer (XRD) and the scanning electron microscope (SEM) image was used for the structural elucidation and surface morphology confirmation. Using LOT-ORAL solar simulator, current density–voltage, *J–V* characteristic after standardizing with Si photodiode to 100 mW/cm$^2$ was measured. The Sandwich-type cells (1 cm$^2$) were prepared by sealing together the ZnO-coated electrode which was further scratched to obtain an active area of 0.25 cm$^2$; with the counter electrode using a transparent film of Surlyn 1472 polymer. The electrolyte was then introduced through holes drilled in the counter electrode, which were sealed immediately with microscope cover slides and additional strips of Surlyn to avoid leakage unless otherwise stated. It is scientifically recommended to use a photo-mask to cover the photo-cell in order to define the accurate active area, but in our case we scratch the entire film to limit the active area to only 0.25 cm$^2$ and the non-active region is meticulously sealed using a non-reflecting Surlyn polymer tape. The impedance spectroscopy measurement (EIS) was performed using BAS-Zahner IM6 Impedance analyzer. For IPCE measurement, cell of maximum conversion efficiency performance was standardized with UV filtered Si diode before actual measurement wherein light was focused from the glass side.

## 3. Results and discussion

Fig. 1a shows the ZnO X-ray diffraction pattern wherein the *c*-axis growth, i.e. compared to neighboring (1 1 0) and (1 0 1) peaks (0 0 2) reflection plane showed relatively weak intensity which is related to the relative growth rates of various faces as intermolecular bonding preferences or dislocations, supersaturation, temperature, solvents and surfactant, sculptures the surface morphology and the structural related aspects of any domain [22]. A weak (0 0 2) reflection plane in the ZnO NPs XRD pattern suggested, indirectly, the presence of higher oxygen vacancies. In general, oxygen vacancies and interstitial zinc atoms have strong influence on the electronic properties of ZnO as electrons in ZnO are located in the conduction band and/or shallow traps [23]. In short, higher the number of oxygen vacancies lower is the resistivity. Fig. 1b presents the high resolution SEM image of ZnO NPs wherein surface texture was smooth and uniform without pinholes, cracks and defects over the whole respective surface image. Individual ZnO crystal was close to 100 nm in diameter. Several small spherical crystallites of 20–30 nm in diameters were agglomerated to form relatively bigger island. These irregular (sizes and shapes) crystallites would be practically important for light scattering and dye-absorbing effect to enhance DNSCs performance. Fig. 2a shows the chemical structure of the D102 dye. Very strong absorption coefficient (55,800 L mol$^{-1}$ cm$^{-1}$ at 491 nm), about four times stronger than the ruthenium N3 dye (13,900 L mol$^{-1}$ cm$^{-1}$ at 541 nm), was obtained [24]. The higher extinction coefficient of dye and mesoporous ZnO NPs of angular sizes would be interesting when used in DNSCs applications. For J-V characteristics, 15 mL of methoxyacetonitrile (98%) containing 0.6 M 1-hexyl-2-3-dimethylimidazolium iodide (C6DMI), 0.1 M lithium iodide (LiI), 0.05 M iodide ($I_2$), and 0.5 M 4-*tert*-butylpyridine (*t*-BPy) solution was used as an electrolyte. All measurements were carried

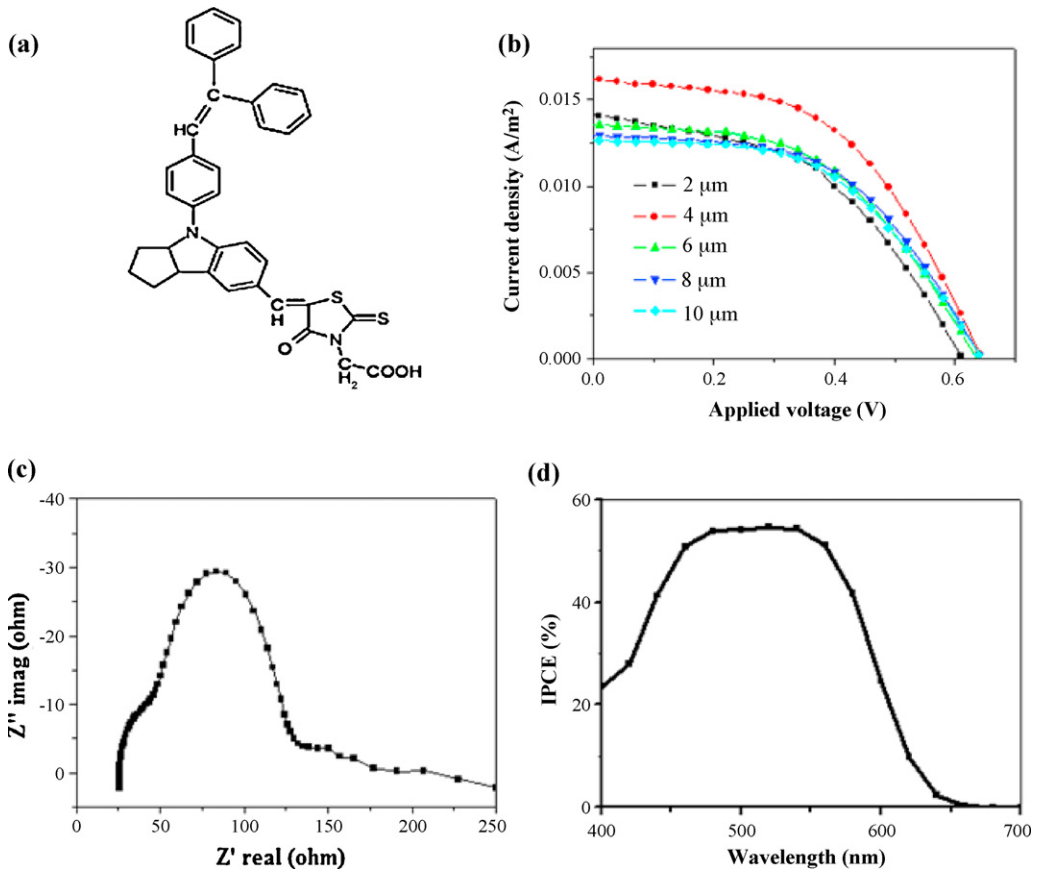


**Fig. 2.** (a) Chemical structure of indoline D102 dye, (b) change in *J–V* with ZnO NPs thicknesses, and (c and d) typical Nyquist and IPCE curves for ZnO NPs electrode that showed maximum performance.

out under AM 1.5 Sun light intensity, i.e. 100 mW/cm$^2$. Five ZnO electrodes (*viz* 2–10 μm thicknesses as previously discussed) with 2 μm thickness interval were immersed in D102 dye for 1 h. There was no formation of insulating surface aggregation $Zn^{2+}$/dye layer that generally limits the cell performance. The dye amount loaded in different electrodes were $5.40 \times 10^{-6}$, $4.18 \times 10^{-6}$, $9.40 \times 10^{-5}$, $8.2 \times 10^{-5}$ and $4.4 \times 10^{-5}$ mol cm$^{-2}$, respectively. All electrodes show excellent, better than all our previous measurements [12–15], performances. As depicted in Table 1, irrespective of electrode thickness, the $J_{sc}$ value in all electrodes was above 10 mA/cm$^2$, indicating that the D102 dye molecules are active for electrons injection in ZnO NPs. The ZnO NPs-D102 photoelectrode of 4 μm thickness exhibited a very impressive $J_{sc}$ of 17.43 mA/cm$^2$ and an appreciable $V_{oc}$ of 0.63 V. This could be due to two reasons; high molar extinction coefficient of the dye that penetrates deep into the ZnO NPs matrix and the formation of the packed layers by the dye molecules on the surface of the ZnO NPs which generally leads to a better blocking of the dark current, and hence a higher $V_{oc}$. Secondly, ZnO NPs-dye hetero-junction must be free from the insulating agglomeration layer that could have enabled fast charge transport and thereby higher photocurrent. The obtained competitive $V_{oc}$ could be a result of the particle size and the dye dipole moment. Particle size influence is widely known as larger particles with lower internal surface areas harvest more photons relative to smaller particles and the influence of the dipole moment on the rectifying behavior was investigated by using various benzoic acids with different dipole moments [25]. Increase in electrode thickness reduced the performance in a small amount without much decrease in $V_{oc}$. Fixed $V_{oc}$ value supported for good interfacial stability between ZnO NPs and dye molecules. Because of the strong molar extinction coefficient of this dye, a film of thickness of 4 μm was sufficient to achieve an efficiency of 5.4%. The high molar extinction coefficient of organic dyes could be ideal absorber for nanostructured DNSCs. This electrode possessed a *ff* of 48.2%. With further increase in electrode thickness there was decrease in fill factor from 51 to 43% due to increase in electrode series resistance, a function of electrode thickness. This is attributed to impact of diffusion length and life time of photo-injected electrons. If diffusion length (thickness) is higher than electron life time, then electron follows the recombination mechanism with reduced current density. In Fig. 2c, the Nyquist curve, obtained from an impedance spectroscopy measurement for optimal ZnO NPs electrode of 4 μm thickness in dark, showed two distinct semicircular loops in the high frequency range and in the low-frequency range; the third semicircular loop was partially observed in the figure. The smaller semicircular loop in the high frequency region was caused by the counter electrode–electrolyte interfacial charge transfer resistance and the second semicircular loop was due to the working electrode–electrolyte interfacial resistance, i.e. the recombination resistance, which was, in fact, higher, resulted in higher $V_{oc}$. The initial lag in high frequency region can be considered to be the sheet resistance offered by the transparent conducting oxide [26].

**Table 1**
Nanocrystalline ZnO photoelectrode thickness impact on *J–V* performance.

| ZnO photoelectrode thickness (±0.2) μm | $V_{oc}$ (V) | $J_{sc}$ (mA/cm$^2$) | *ff* (%) | $\eta$ (%) |
|---|---|---|---|---|
| 2 | 0.64 | 13.66 | 51.6 | 4.35 |
| 4 | 0.637 | 17.43 | 48.2 | 5.44 |
| 6 | 0.612 | 14.17 | 47.0 | 4.089 |
| 8 | 0.612 | 14.04 | 44.9 | 3.56 |
| 10 | 0.595 | 13.87 | 43.0 | 3.55 |

In Fig. 2d, IPCE spectrum of D102-dye immobilized ZnO NPs electrode of 4 μm thickness is presented wherein, electrode exhibited competitive but certainly less than other reports 60% IPCE revealing that there is a need for the systematic efforts for improving the *ff* and $V_{oc}$ by coating a (buffer) layer of other wide band gap semiconductors such as $SiO_2$, $Al_2O_3$ or $ZrO_2$, etc. [27,28], which is underway.

## 4. Conclusions

Concisely, this communication provides a broad insight of use of organic based indoline D102 dye as an efficient sensitizer for obtaining nearly 17.7 mA/cm$^2$ current density with power conversion efficiency close to 5.4%, one of the competitive results than previously tested ruthenium-based sensitizers for ZnO nanoparticles-based dye cells which is attributed to increased absorption of light as a result of higher extinction coefficient of the dye. For designing solid state solar cells in the presence of Spiro, or P3HT, hole transporting materials for ZnO system this combination would be the best choice. Formation of core-shell structure might even increase the fill factor followed by open circuit voltage therefore device conversion performance, is underway.

## Acknowledgements

Authors are greatly thankful to projects; (a) a grant from the cooperative R&D Program (B551179-08-03-00) funded by the Korea Research Council Industrial Science and Technology, Republic of Korea, (b) 'Hydrogen Energy R&D Center', one of the 21st century frontiers R&D program funded by Ministry of Science and Technology of Korea, and (c) National Research Foundation of Korea (NRF) funded by the Korea government (MEST) (Grant 2010-0028717), for the financial assistance.

## References

[1] B. O'Regan, M.A. Gratzel, A low-cost, high-efficiency solar cell based on dye-sensitized colloidal $TiO_2$ films, Nature 353 (1991) 340–737.
[2] M.K Nazeeruddin, A. Kay, I. Rodicio, R. Humphry Baker, E. Muller, P. Liska, et al., Conversion of light to electricity by cis-X2bis(2,2′-bipyridyl-4,4′-dicarboxylate)ruthenium(II) charge-transfer sensitizers (X = $Cl^-$, $Br^-$, $I^-$, $CN^-$, and $SCN^-$) on nanocrystalline titanium dioxide electrodes, J. Am. Chem. Soc. 115 (1993) 6382–6390.
[3] A. Hagfeldt, M. Gratzel, Light-induced redox reactions in nanocrystalline systems, Chem. Rev. 95 (1995) 49–68.
[4] A. Hagfeldt, M. Gratzel, Molecular photovoltaics, Acc. Chem. Res. 33 (2000) 269–277.
[5] Q. Zhang, C.S. Dandeneau, X. Zhou, G. Cao, ZnO nanostructures for dye-sensitized solar cells, Adv. Mater. 21 (2009) 4087–4108.
[6] I. Gonzalez-Valls, M. Lira-Cantu, Vertically-aligned nanostructures of ZnO for excitonic solar cells: a review, Energy Environ. Sci. 2 (2009) 19–34.
[7] C.-Y. Chen, M.-W. Chen, J.-J. Ke, C.-A. Lin, J.R.D. Retamal, J.-H. He, Surface effects on optical and electrical properties of ZnO nanostructures, Pure Appl. Chem. 82 (2010) 2072–2255.
[8] X. Sheng, J. Zhai, L. Jiang, D. Zhu, Enhanced photoelectrochemical performance of ZnO photoanode with scattering hollow cavities, Appl. Phys. A: Mater. Sci. Process. 96 (2009) 473–479.
[9] Y.J. Shin, J.H. Lee, J.H. Park, N.G. Park, Enhanced photovoltaic properties of $SiO_2$-treated ZnO nanocrystalline electrode for dye-sensitized solar cell, Chem. Lett. 36 (2007) 1506–1507.
[10] K. Keis, E. Magnusson, H. Lindstrom, S.E. Lindquist, A. Hagfeldt, A 5% efficient photo electrochemical solar cell based on nanostructured ZnO electrodes, Sol. Energy Mater. Sol. Cells 73 (2002) 51–58.
[11] A. Tsukazaki, A. Ohtomo, T. Onuma, M. Ohtani, T. Makino, M. Sumiya, et al., Repeated temperature modulation epitaxy for p-type doping and light-emitting diode based on ZnO, Nat. Mater. 4 (2005) 42–46.
[12] S. Yodyingyong, Q. Zhang, K. Park, C.S. Dandeneau, X. Zhou, D. Triampo, et al., ZnO nanoparticles and nanowire array hybrid photoanodes for dye-sensitized solar cells, Appl. Phys. Lett. 96 (2010), 073115(1–3).
[13] R.S. Mane, H.M. Nguyen, T. Ganesh, S.B. Ambade, N. Kim, S.H. Han, A novel HMP-2 dye of high extinction coefficient designed for enhancing the performance of ZnO platelets, Electrochem. Commun. 11 (2009) 752–755.
[14] H.M. Nguyen, R.S. Mane, T. Ganesh, S.H. Han, Aggregation-free ZnO nanocrystals coupled HMP-2 dye of higher extinction coefficient for enhancing energy conversion efficiency, J. Phys. Chem. C 113 (2009) 9206–9209.
[15] T. Ganesh, R.S. Mane, G. Cai, J.H. Chang, S.H. Han, ZnO nanoparticles–CdS quantum dots/N3 dye molecules: dual photosensitization, J. Phys. Chem. C 113 (2009) 7666–9669.
[16] M. Gratzel, Applied physics – solar cells to dye for, Nature 421 (2003) 586–587.
[17] F. De Angelis, S. Fantacci, A. Selloni, M. Gratzel, M.K. Nazeeruddin, Influence of sensitizer's dipole on open-circuit potential of the dye-sensitized solar cell, Nano Lett. 7 (2007) 3189–3193.
[18] M.K. Nazeeruddin, F. De Angelis, S. Fantacci, A. Selloni, G. Viscardi, P. Liska, et al., Combined experimental and DFT-TDDFT computational study of photoelectrochemical cell ruthenium sensitizers, J. Am. Chem. Soc. 127 (2005) 16835–16847.
[19] S. Ito, S.M. Zakeeruddin, R. Humphry-Baker, P. Liska, R. Charvet, P. Comte, et al., High-efficiency organic-dye-sensitized solar cells controlled by nanocrystalline-$TiO_2$ electrode thickness, Adv. Mater. 18 (2006) 1202–1205.
[20] K. Hara, Z.S. Wang, T. Sato, A. Furube, R. Katoh, H. Sugihara, et al., Oligothiophene-containing coumarin dyes for efficient dye-sensitized solar cells, J. Phys. Chem. B 109 (2005) 15476–15482.
[21] S.L.S. Seow, A.S.W. Wong, V. Thavasi, R. Jose, S. Ramakrishna, G.W. Ho, Controlled synthesis and application of ZnO nanoparticles, nanorods and nanospheres in dye-sensitized solar cells, Nanotechnology 20 (2009) 45604–45609.
[22] X.L Chen, B.H. Xu, J.M. Xue, Y. Zhao, C.C. Wei, J. Sun, et al., Boron-doped zinc oxide thin films for large-area solar cells grown by metal organic metal vapor deposition, Thin Solid Films 515 (2007) 3753–3759.
[23] S. Alex, U. Santhosh, S. Das, Dye sensitization of nanocrystalline $TiO_2$: enhanced efficiency of unsymmetrical versus symmetrical squaraine dyes, J. Photochem. Photobiol. A: Chem. 172 (2005) 63–71.
[24] T. Horiuchi, H. Miura, S. Uchida, Highly-efficient metal-free organic dyes for dye-sensitized solar cells, Chem. Commun. 24 (2003) 3036–3037.
[25] J. Kruger, U. Bach, M. Gratzel, Modification of $TiO_2$ heterojunctions with benzoic acid derivatives in hybrid molecular solid-state devices, Adv. Mater. 12 (2000) 447–451.
[26] M. Wang, P. Chen, R. Humphry-Baker, M. Zakeeruddin, M. Gratzel, The influence of charge transport and recombination on the performance of dye-sensitized solar cells, Chem. Phys. Chem. 10 (2009) 290–299.
[27] E. Palomares, J.N. Clifford, S.A. Haque, T. Lutz, J.R. Durrant, Control of charge recombination dynamics in dye sensitized solar cells by the use of conformally deposited metal oxide blocking layers, J. Am. Chem. Soc. 125 (2003) 475–482.
[28] D.B. Menzies, Q. Dai, L. Bourgeois, R.A. Caruso, Y.B. Cheng, G.P. Simon, et al., Modification of mesoporous $TiO_2$ electrodes by surface treatment with titanium(IV), indium(III) and zirconium(IV) oxide precursors: preparation, characterization and photovoltaic performance in dye-sensitized nanocrystalline solar cells, Nanotechnology 18 (2007) 125608–125618.